J Mater Sci (2010) 45:5054–5060
DOI 10.1007/s10853-010-4456-x

ICAM 2009

Preparation of conducting polyanilines doped with Keggin-type polyoxometalates and their application as counter electrode in dye-sensitized solar cells

Luiz C. P. Almeida · Agnaldo D. Gonçalves · João E. Benedetti · Paulo C. M. L. Miranda · Luís C. Passoni · Ana F. Nogueira

Received: 30 November 2009 / Accepted: 29 March 2010 / Published online: 15 April 2010

Abstract Conducting polyanilines doped with two Keggin-type polyoxometalates (POMs) were synthesized by chemical oxidation of aniline. Both conducting polymers provided electrical conductivity values up to 0.1 S cm^{-1}, as measured by the standard four-probe technique. Structural and morphological characterizations for these materials were achieved by FTIR spectra, X-ray diffraction, scanning electron microscopy (SEM), and thermogravimetric analysis. These conducting polyanilines doped with Keggin-type polyoxometalates (PANI–POMs) were also used to prepare a new type of counter electrode for application in dye-sensitized solar cells (DSCs). Promising results were achieved from DSCs based on PANI–POMs as the materials for the counter electrode, which provides evidence for the dopant role in enhancing the electrical conductivity of PANI.

L. C. P. Almeida · A. D. Gonçalves · J. E. Benedetti · P. C. M. L. Miranda · A. F. Nogueira (✉)
Institute of Chemistry, University of Campinas—UNICAMP, P.O. Box 6154, 13083-970 Campinas, SP, Brazil
e-mail: anaflavia@iqm.unicamp.br

L. C. P. Almeida
e-mail: lalmeida@iqm.unicamp.br

A. D. Gonçalves
e-mail: agnaldosg@gmail.com

J. E. Benedetti
e-mail: jebenedetti@iqm.unicamp.br

P. C. M. L. Miranda
e-mail: miranda@iqm.unicamp.br

L. C. Passoni (✉)
Laboratório de Ciências Químicas/CCT, Universidade Estadual do Norte Fluminense—UENF, 28013-612 Campos dos Goytacazes, RJ, Brazil
e-mail: lpassoni@uenf.br

Introduction

Among the most technologically promising conducting polymers polyaniline (PANI) stands out because of its high environmental stability, low cost, versatility and processibility, good conductivity, and unique electro, optical, and electrochemical properties [1]. The combination of these properties makes PANI and its derivatives useful for various applications including rechargeable batteries [2, 3], supercapacitors [4, 5], light emitting diodes [6], transistors [7], molecular sensors [8], nonlinear optical devices [9], corrosion protection [10, 11], electromagnetic interference shielding [12], electrochromic displays [13], and photovoltaic devices [14]. The properties of PANI and other conducting polymers depend on their microstructure and morphology, and these are determined by the synthesis method, counter-anions, presence of structural defects, cross-linking, and other variables that are very difficult to control simultaneously [15]. The demand for these materials, endowed with a wide range of desirable properties, is always increasing. One of the techniques to develop such materials is the formulation of composites from compatible materials individually possessing the desirable properties. PANI blends and composites have been prepared mostly via the chemical oxidation route [16], although electrochemical synthesis was also employed in some cases [17, 18]. In particular, a PANI hybrid material has been prepared using polyoxometalates (POMs) [19]. POMs are currently of great interest mainly due to their interesting nanosized structures [20] and their potential applications in catalysis, conductivity, photoelectrochromic devices, and

molecular electronics [21]. The versatility presented by the POMs, including the Keggin-type, is due to their attractive physical and chemical properties, such as thermal stability, reversible multielectron electrochemical reactions, and photoelectrochemical properties, which make them structural and functional models for nanometric oxide particles [22–24]. Recent study has shown that POMs can be incorporated into conducting organic polymers during chemical or electrochemical polymerization. Pozniczek et al. [24, 25] and Hasik et al. [26–28] demonstrated that the insertion of POMs into polyacetylene, polypyrrole, and PANI produces a new type of catalyst with potential applications in electrocatalysis and other relevant applications [29, 30].

Among various applications for conducting polymers, their use in counter electrodes for dye-sensitized solar cells (DSCs) has recently attracted attention. The DSCs usually consist of two conducting transparent electrodes in a sandwich configuration, separated by liquid electrolyte containing the I^-/I_3^- redox couple [31]. In general, the working electrode consists of a dye-sensitized porous nanocrystalline TiO_2 thick film and the counter electrode of a platinized conducting substrate to catalyze redox couple regeneration. However, the cost of platinum is quite high, which limits somehow its widespread application in DSCs. In order to reduce the production cost of these devices, the application of carbon-based materials such as carbon nanotubes [32] and conducting polymers has deserved some recent attention [33]. In addition, the lower cost of conducting polymers such as PANI provides interesting advantages, as mentioned before, beyond the catalytic activity for I_3^- reduction [34].

In this study, we report the preparation and characterization of two distinct conducting PANI from the incorporation of POMs into the polymer matrix during the chemical polymerization of aniline, where the POM molecules $H_3PMo_{12}O_{40}$ and $H_3PW_{12}O_{40}$ act as acids in the reaction media, as well as dopants in the final PANI. The PANI–POM compounds synthesized in this study were also used to prepare counter electrodes to be applied in DSCs. The mixture of PANI–POM compounds, ZnO nanoparticles, and carbon black is an interesting approach to provide catalytic properties for the reduction of triiodide ions to iodide ions, the main redox couple present in DSCs.

Experimental

Materials

All chemicals and solvents in this study were of analytical grade, and used as received from Synth and Tedia. Aniline was distilled under reduced pressure and stored in the dark below 4°C before using.

Preparation of $H_3PMo_{12}O_{40}$ and $H_3PW_{12}O_{40}$

$H_3PMo_{12}O_{40}$ and $H_3PW_{12}O_{40}$ were synthesized in a similar manner from their respective oxoanion salts ($NaMoO_4 \cdot 2H_2O$ and $NaWO_4 \cdot 2H_2O$) and phosphoric acid (H_3PO_4) [35]. First, the oxoanions (42 mmol) were dissolved in 100 mL of deionized water followed by addition of 3.5 mmol of 85% phosphoric acid. The resulting solutions were acidified to reach pH 2 by addition of concentrated sulfuric acid and heated under reflux at 70 °C for 1 h. The solutions containing the POMs were transferred to a separation funnel with 100 mL of ethyl ether. After addition of concentrated sulfuric acid (~30 mL), the POMs were extracted in ethyl ether. Water was added and the ethyl ether was evaporated. Finally, $H_3PMo_{12}O_{40}$ and $H_3PW_{12}O_{40}$ were obtained after recrystallization and used soon after.

Preparation of insulating PANI

The PANI was prepared by chemical polymerization of aniline using $(NH_4)S_2O_8$ as the oxidant as described by Manohar et al. [36]. The synthesized polymer (emeraldine salt) was treated with a 1 mol L^{-1} NH_4OH solution for 24 h under constant stirring at room temperature.

Preparation of conducting PANI–POMs

Freshly distilled aniline (10.6 mmol), and 3.3 mmol of the POM ($H_3PMo_{12}O_{40}$ or $H_3PW_{12}O_{40}$) were dissolved in 30 mL of acetonitrile. Simultaneously 2.01 g (8.8 mmol) of ammonium persulfate was dissolved in 3.0 mL of deionized water and slowly added dropwise to the aniline–POM–acetonitrile solution. The synthesis was carried out at room temperature with constant stirring for 24 h. After this time, the formation of a dark precipitate was observed, which was removed by filtration, and alternately washed with acetone and deionized water until a completely colorless filtrate was obtained. The precipitate was then dried at 50 °C until constant mass. The products related to $H_3PMo_{12}O_{40}$ and $H_3PW_{12}O_{40}$ were named PANI–Mo and PANI–W, respectively.

Characterization of PANI–POMs

The products were characterized by FTIR measurements performed on a Shimadzu 8300 instrument with the sample dispersed in KBr pellets. X-ray diffraction (XRD) measurements were recorded on an XRD instrument (Rigaku Rotaflex RU 200B), employing monochromatized Cu K_α incident radiation. Scanning electron microscopy (SEM) images were obtained on a Hitachi S-570 scanning electron microscope operating at 20 kV. Thermal studies of the

materials were carried out using a thermal analysis instrument (TA Instruments 2920 TGA-DSC). Samples were subjected to a constant heating rate of 10 °C/min under nitrogen flow. Electrical conductivity (dc) measurements were performed at ambient temperature using the four-probe method with a Cascade Microtech C4S-64 probe connected to 617 Keithley electrometer and a digital multimeter Minipa ET-2500. The PANI–POM samples were pressed into pellets (ca. 2 cm of diameter and 2 mm of thickness) by applying a pressure of 50 kN.

Preparation of counter electrode

The counter electrodes were prepared from a slurry obtained by mixing 60 mg of PANI–POM (PANI–Mo or PANI–W) material, 150 mg of ZnO powder, 1.5 mL of deionized water, and 6.0 mg of carbon black. The resulting mixture was ground in a mortar for ca. 1 h. The slurry was then applied on the conducting substrate (fluorine-doped SnO_2 glass) by the doctor blading technique. Transparent tape (Scotch®) was used as frame and spacer. The resulting film was dried at 150 °C for 30 min to provide adequate electrical contact between the particles.

Solar cell assembly and characterization

The photoanode was prepared using a TiO_2 suspension (Solaronix) deposited by the doctor blading technique onto the conducting substrate. The resulting film was submitted to heat treatment at 450 °C for 30 min. The thickness of the porous nanostructured semiconductor layer is about ~7 μm, measured with a Tencor Alpha-step 200 profilometer. The electrodes were then immersed, while still warm (ca. 80 °C), into a 0.25 mmol L^{-1} ethanolic solution of the complex *cis*-bis(isothiocyanato)bis(2,2′-bipyridyl-4,4′-dicarboxylate-ruthenium (II) bis-tetrabutylammonium (also known as N-719, Solaronix) and remained in this solution for 12 h at room temperature. Then, the sensitized films were rinsed with absolute ethanol to remove nonadsorbed N-719 species and allowed to dry in air.

The liquid electrolyte was composed of 0.1 mol L^{-1} LiI, 0.05 mol L^{-1} I_2, 0.8 mol L^{-1} tetrabutylammonium iodide, 0.5 mol L^{-1} 4-*tert*-butylpyridine in 50% acetonitrile, and 50% 3-methoxypropionitrile. The DSCs were sealed by using the thermoplastic film Surlyn 1472 (DuPont). The electrolyte was introduced through holes drilled in the counter electrode, which were sealed immediately with thermoplastic and a glass slide. The *J–V* curves were measured under standard AM 1.5 conditions using a 150-W Xe lamp as the light source. The measurements were carried out under 100 mW cm^{-2}, monitored by using a silicon photodiode from Newport Optical Power Meter, model 1830-C. The data from the *J–V* measurements represent the average behavior for at least three DSCs of the same sample. The average DSC geometrical area was 0.25 cm^2, measured by using a magnifying lens.

Results and discussion

FTIR spectral analyses

The FTIR spectra in the frequency range 2,500–400 cm^{-1} are shown in Fig. 1 for insulating PANI and its conducting forms PANI–Mo and PANI–W.

For the two conducting materials PANI–Mo and PANI–W, prominent peaks in the region 1,100–1,600 cm^{-1} resemble the reported spectrum of PANI [37]. The incorporation of Keggin structures of POMs into the polymer matrix was confirmed by presence of characteristics peaks in the region 800–1,100 cm^{-1}. All peaks are shown in Table 1 [20]. The bands of PANI in PANI–Mo and PANI–W also showed a slight shift in comparison to bulk PANI, suggesting a substantial interaction between the polymer and POMs occurs.

The spectra of PANI–Mo and PANI–W show also peaks at 1,149 and 1,142 cm^{-1}, which are characteristics of charge delocalization of the conductive form of PANI [33]. These peaks are directly correlated with the electrical conductivity, which is several orders of magnitude higher for PANI–Mo and PANI–W (0.1 S cm^{-1} for both materials) than insulating PANI (~10^{-9} S cm^{-1}).

X-ray diffraction studies

X-ray diffraction patterns recorded for the insulating PANI and conducting PANI–POMs composites are shown in Fig. 2. The undoped PANI (Fig. 2a) presents an amorphous nature with two characteristic broad peaks at 2θ around 20° and 25° [38], which indicates the low degree of crystallinity of the material.

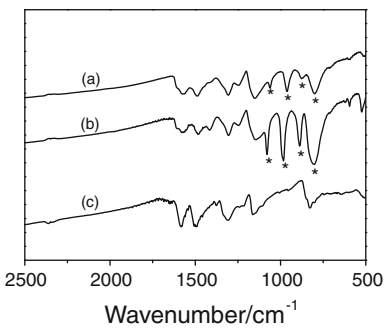

Fig. 1 FTIR spectra of (*a*) PANI–Mo, (*b*) PANI–W, and (*c*) PANI. (*) indicates the polyoxometalates peaks

Table 1 FTIR peak values and their assignments for PANI and PANI–POMs materials

PANI (cm^{-1})	PANI–Mo (cm^{-1})	PANI–W (cm^{-1})	Peaks of	Assignment
1,583	1,576	1,579	PANI	Stretching of quinoid ring
1,498	1,489	1,483	PANI	Stretching of benzenoid ring
1,309	1,308	1,306	PANI	C–N stretching + C–C bending
1,242	1,249	–	PANI	C–N stretching + C–C stretching
–	1,149	1,142	PANI	$Q{=}NH^{+}{=}Q–$; $–B–NH^{+}{\cdot}–B–$
–	1,063	1,080	POM	Stretching P–O
–	962[a]	983[b]	POM	Stretching (Mo = O[a], W = O[b])
–	870[c]	887[d]	POM	Asymm. stretch (Mo–O–Mo[c], W–O–W[d])
–	800[e]	802[f]	POM	Sym. stretch (Mo–O–Mo[e], W–O–W[f])

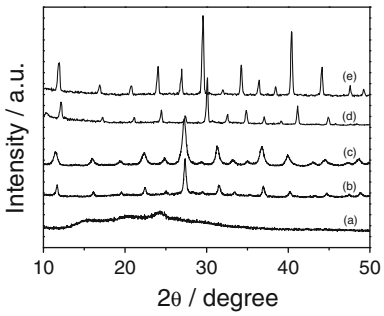

Fig. 2 X-ray pattern of (*a*) PANI, (*b*) PANI–Mo, (*c*) PANI–W, (*d*) $H_3PMo_{12}O_{40}$, and (*e*) $H_3PW_{12}O_{40}$

On the other hand, the PANI–Mo and PANI–W show characteristic peaks of their respective doping agent POMs, indicating higher crystallinity compared to insulating PANI, as can be seen in Fig. 2b. These peaks also suggest that the POMs are not molecularly dispersed into the polymer matrix, but as agglomerates formed from its secondary and tertiary structures. These secondary and tertiary structures are formed probably due to the interaction of the POM with the amine groups of PANI. POMs are known to present strong interactions with amines or ammonia [31].

SEM analysis

In order to investigate the morphological properties in more detail, the insulating PANI and conducting PANI–POMs were characterized by SEM. The SEM images were basically formed by the secondary electrons emitted from the surface layers, as can be seen from Fig. 3. The insulating PANI film has relatively large agglomerates with a smoothened aspect containing small fibers in between (Fig. 3a). The small (nano and micro) fibers are 1D structures, which are commonly observed for PANI [39]. However, the use of POM as acid doping agents in the polymeric matrix, instead of the usual inorganic acids such as HCl or H_2SO_4, assists chain secondary growth, which results in polymer chain agglomerates with granular shape, as may be seen in Fig. 3b and c for PANI–Mo and PANI–W, respectively.

Thermal analysis

Thermogravimetric curves of insulating PANI and the PANI–POM under nitrogen flow are showed in Fig. 4. All samples revealed a relatively small weight loss at about 90 °C. It is interesting to note that insulating PANI (pure) always contains adsorbed water and other solvents from the synthesis. Hence, the small weight loss cannot be directly related to polymer degradation but should be associated with slow release of water and solvent molecules. The insulating PANI showed a remarkable weight loss at about 450 °C that corresponds to PANI degradation, and at 600 °C the weight loss reaches 35%.

Unlike insulating PANI, the curve for PANI–Mo showed a small weight loss starting at 250 °C that can be attributed to the first steps of degradation of PANI chains. A large weight loss of around 50% was observed at 650 °C, which is related to the degradation of organic framework and also to the degradation of the $H_3PMo_{12}O_{40}$ molecules. The curve for PANI–W also showed a slight weight loss at 250 °C, as observed for PANI–Mo. Nevertheless, the majority weight loss was observed close to 800 °C, showing that PANI–W is more thermally stable than PANI–Mo. Therefore, the PANI–W is more stable than PANI–Mo, even both materials had the same spectroscopic, electrical, and morphological characteristics. This is in good agreement with the fact that W-containing POMs are more stable than the Mo-containing ones, as may be seen in Fig. 4.

Solar cell characterization

The electrical properties of PANI–POM materials in conjunction with the catalytic activity of carbon-based materials would be of interest for replacing platinum in counter electrodes for DSCs. In this study, the counter electrode

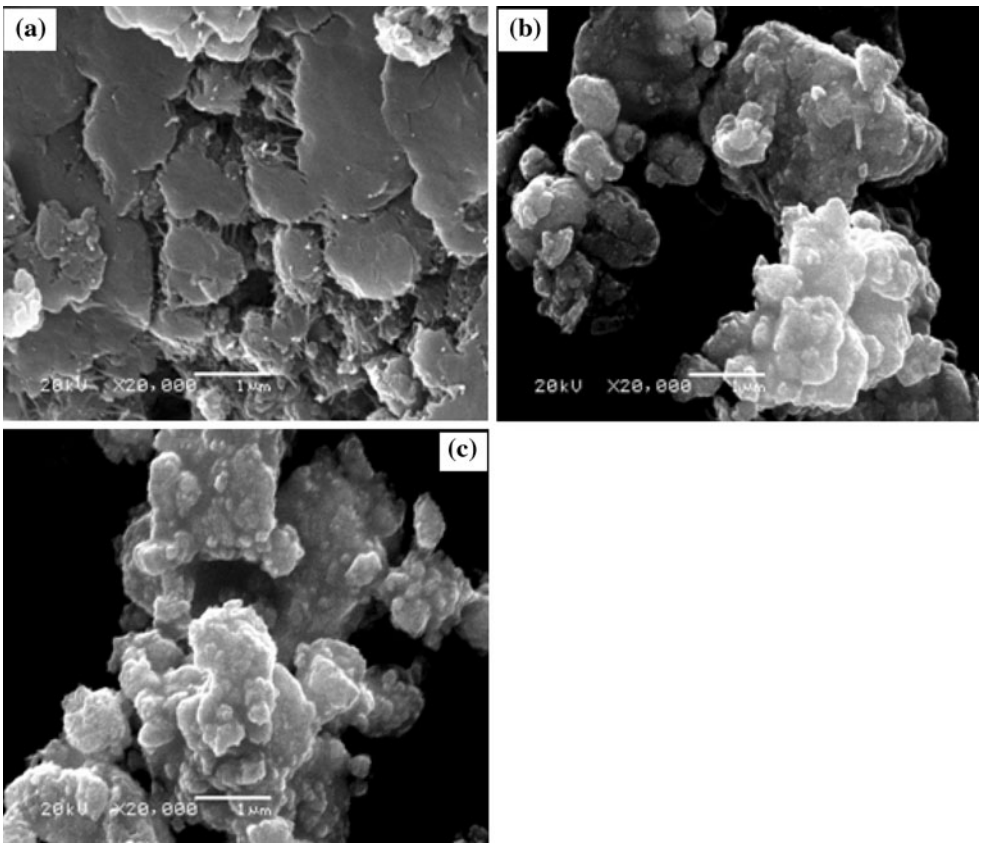

Fig. 3 SEM images of **a** PANI, **b** PANI–Mo, and **c** PANI–W

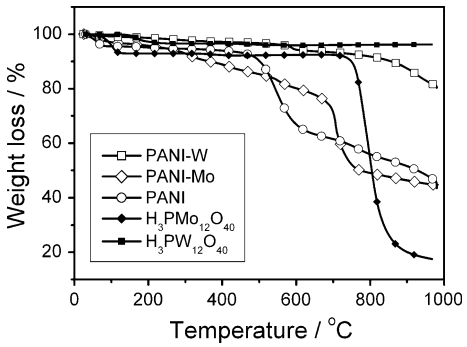

Fig. 4 Thermogravimetric curves of samples analyzed at 10 °C min^{-1} under a N_2 atmosphere

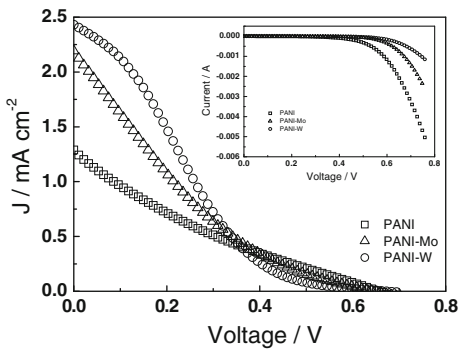

Fig. 5 *J–V* curves (AM1.5, illumination intensity of 100 mW cm^{-2}) of the DSCs based on the composite materials as the counter electrode. The active area was ca. 0.25 cm^2. The *inset* shows the dark *J–V* curves

was prepared from a slurry containing carbon black, whose function was to enhance the electrical conductivity and catalytic activity of the electrode; ZnO nanoparticles were used to increase the surface area of the resulting porous films. The application of PANI–POM materials as the counter electrodes in DSCs provided promising photoelectrochemical properties, as may be seen in Fig. 5.

The photocurrent–voltage characteristics from Fig. 5 are summarized in Table 2. The application of PANI as the composite film in counter electrodes for DSCs resulted in promising photocurrent values (Table 2). However, when the PANI–POM materials were applied as the catalytic layers in the counter electrode, a ca. twofold increase in photocurrent was observed. This result provided evidence for the enhanced electrical conductivity of the doped materials. The V_{oc} values were relatively high (Table 2), but there are considerable recombination losses. Despite the poor fill factor (FF) values, arising mainly from the high series resistance, relatively high photocurrent densities (up to 2.5 mA cm^{-2}) could be achieved by using

Table 2 Performance characteristics from the *J–V* curves of the DSCs based on the composite materials as the catalytic layer in the counter electrodes

DSC	J_{sc} (mA cm^{-2})	V_{oc}/V	FF	Efficiency (%)
PANI–W	2.43	0.70	0.17	0.29
PANI–Mo	2.19	0.64	0.14	0.21
PANI	1.28	0.64	0.18	0.15

The illumination intensity was 100 mW cm^{-2} (AM1.5) and active area of the solar cells ca. 0.25 cm^2

PANI–POM as the catalytic layer for the counter electrode in the DSCs. The high values of current observed in dark *J–V* curves reveal the existence of remarkable charge recombination process. This is a consequence of a high series resistance of the electrodes, low porosity, and less active sites when compared to platinum electrode. These effects influence directly the efficiency of our solar cells as observed in other reports [40–42].

The optimization of the catalytic layer based on the composite material studied herein is expected to improve the FF and efficiency (η) values by increasing the surface area of the counter electrode. Such optimization studies are underway in our laboratory, especially in light of the promising thermal stability properties of the PANI–POMs studied in this work.

Conclusion

The preparation and structural, electrical, and morphological properties of PANI doped with Keggin-type POMs were evaluated in this study. FTIR analyses showed an effective incorporation of POM molecules into the PANI matrix. POMs acted as doping agents and have improved the electrical conductivity of PANI–POM-based materials. XRD indicated a higher crystallinity for the PANI–POM materials compared to PANI, and this may be attributed to the presence of POM molecules that posses high crystallinity. Remarkable morphological differences were observed by SEM analysis. Thermogravimetric analysis indicated higher thermal stability for the PANI–POM compared to PANI, and it may be related to the stability presented by POM molecules. It is important to note that the PANI–POM materials presented high electrical conductivities, about 0.1 S cm^{-1} for both (PANI–Mo and PANI–W), and this was one of the reasons to apply these materials as counter electrodes. The results presented herein demonstrated the applicability of the PANI–POM material as counter electrodes in DSCs. Devices with current density of 2 mA cm^{-2} and open circuit voltage (V_{oc}) higher than 0.60 V were obtained. Further studies are underway directed at decreasing the series resistance, which affects mainly the FF values.

Acknowledgements The authors acknowledge FAPESP (fellowships 08/53059-4), FAPERJ, and CNPq for the financial support, and Prof. Carol H. Collins for English revision.

References

1. Nalwa HS (1997) Handbook of organic conductive molecules and polymers. Wiley, Chichester
2. Sotomura T, Uemachi H, Takeyama K, Naoi K, Oyama N (1992) Electrochim Acta 37:1851
3. Oyama N, Tatsuma T, Sato T, Sotomura T (1995) Nature 373:598
4. Benedetti JE, Canobre SC, Fonseca CP, Neves S (2008) Electrochim Acta 52:4734
5. Tamai H, Hakoda M, Shiono T, Yasuda H (2007) J Mater Sci 42:1293. doi:10.1007/s10853-006-1059-7
6. Olivati CA, Carvalho AJF, Balogh DT, Faria RM (2006) J Mater Sci 41:2767. doi:10.1007/s10853-006-6123-9
7. Yuan RK, Yang SC, Yuan H, Jiang RL, Qian HZ, Gui DC (1991) Synth Met 41:727
8. Bartlett PN, Birkin PR (1993) Synth Met 61:15
9. Osaheni JA, Jenekhe SA, Vanherzeele H, Meth JS, Sun Y, MacDiarmid AG (1992) J Phys Chem 96:2830
10. Epstein AJ, Smallfield JAO, Guan H, Fahlman M (1999) Synth Met 102:1374
11. Shinde V, Sainkar SR, Gangal SA, Patil PP (2006) J Mater Sci 41:2851. doi:10.1007/s10853-006-2375-7
12. Baek S, Ree JJ, Ree M (2002) J Polym Sci A Polym Chem 40:983
13. Gurunathan K, Murugan AV, Marimuthu R, Mulik UP, Amalnerkar DP (1999) Mater Chem Phys 61:173
14. Fatuch JC, Soto-Oviedo MA, Avellaneda CO, Franco MF, Romão W, De Paoli MA, Nogueira AF (2009) Synth Met 159:2348
15. Zarbin AJG, Maia DJM, De Paoli MA, Alves OL (1999) Synth Met 102:1277
16. Pud A, Ogurtsov A, Korzhenko A, Shapoval G (2003) Prog Polym Sci 28:1701
17. Anand J, Palaniappan S, Sathyanarnayana DN (1998) Prog Polym Sci 23:993
18. Liu XX, Zhang L, Li YB, Bian LJ, Su Z, Zhang LJ (2005) J Mater Sci 40:4511. doi:10.1007/s10853-005-0854-x
19. Romero PG, Chojak M, Gallegos KC, Asensio JA, Kulesza PJ, Pastor NC, Cantú ML (2003) Electrochem Commun 5:149
20. Müller A, Krickemeyer E, Bögge H, Schmidtmann M, Peters F (1998) Angew Chem Int Ed Engl 37:3360
21. Kozhevnikov IV (2002) Catalysts for fine chemical synthesis. Wiley, Chichester
22. Day VW, Klemperer WG (1985) Science 228:533
23. Romero PG, Pastor NC (1996) J Phys Chem 100:12448
24. Pozniczek J, Bajer IK, Zagorska M, Kruczata K, Dyrek K, Bielafiski A, Prod A (1991) J Catal 132:311
25. Pozniczek J, Bielafiski A, Bajer IK, Zagorska M, Kruczata K, Dyrek K, Prod A (1991) J Mol Catal 69:223
26. Hasik M, Prod A, Bajer IK, Pozniczek J, Bielafiski A, Piwowarska Z, Dziembaj R (1993) Synth Met 972:55
27. Hasik M, Turek W, Stochmal E, Lapkowski M, Prod A (1994) J Catal 147:544
28. Hasik M, Polniczek J, Piwowarska Z, Kruczala K, Dziembaj R, Bielafiski A, Prod A (1994) J Chem Soc Faraday Trans 90:2099
29. Romero PG, Cantú ML (1997) Adv Mater 9:144
30. Gong J, Su ZM, Dai ZM, Wang RS, Qu LY (1999) Synth Met 101:751
31. O'Regan B, Grätzel M (1991) Nature 353:737
32. Murakami TN, Grätzel M (2008) Inorg Chim Acta 361:572

33. Li Q, Wu J, Tang Q, Lan Z, Li P, Lin J, Fan L (2008) Electrochem Commun 10:1299
34. Ikegami M, Miyoshi K, Miyasaka T, Teshima K, Wei TC, Wan CC, Wang YY (2007) Appl Phys Lett 90:153122
35. Moffat JB (2001) Metal–oxygen clusters: the surface and catalytic properties of heteropoly oxometalates. Kluwer, New York
36. Manohar SK, MacDiarmid AG, Epstein AJ (1991) Synth Met 41:711
37. Somani PR, Marimuthu R, Mandale AB (2001) Polymer 42:2991
38. Wang S, Tan Z, Li Y, Sun L, Zhang T (2006) Thermochim Acta 441:191
39. Huang JX, Kaner RB (2006) Chem Commun 367
40. Muto T, Ikegami M, Kobayashi K, Miyasaka T (2007) Chem Lett 36:804
41. Cha SI, Koo BK, Seo SH, Lee DY (2010) J Mater Chem 20:659
42. Suzuki K, Yamaguchi M, Kumagai M, Yanagida S (2003) Chem Lett 32:28